Oscillatory shear-driven gas flows in the transition and free-molecular-flow regimes

Nicolas G. Hadjiconstantinou
Department of Mechanical Engineering, Massachusetts Institute of Technology, Cambridge, Massachusetts 02139

(Received 3 November 2004; accepted 25 January 2005; published online 3 October 2005)

We investigate oscillatory shear-driven gas flows in the transition and free-molecular-flow regimes. Analytical results valid through slip flow and the early transition regime are obtained using a recently proposed, rigorous second-order slip model with no adjustable coefficients. Analytical solution of the collisionless Boltzmann equation provides a description of the high Knudsen number limit ($\mathrm{Kn} \gg 1$) including the bounded shear layers present in the limit of high oscillation frequency. These layers are analogous to the Stokes layers observed in the $\mathrm{Kn} \ll 1$ limit, but contrary to the latter, they exhibit a nonconstant wave speed as demonstrated by Park, Bahukudumbi, and Beskok in Phys. Fluids. **16**, 317 (2004). All theoretical results are validated by direct Monte Carlo simulations. We find that the second-order slip results are in good agreement with direct simulation Monte Carlo (DSMC) solutions up to $\mathrm{Kn} \approx 0.4$; in some cases these results continue to provide useful approximations to quantities of engineering interest, such as the shear stress, well beyond $\mathrm{Kn} \approx 0.5$. The collisionless theory provides, in general, a good description of DSMC results for $\mathrm{Kn} \gtrsim 10$, while in the high frequency limit the agreement is very good for Knundsen numbers as low as $\mathrm{Kn} \approx 5$. © *2005 American Institute of Physics*. [DOI: 10.1063/1.1874193]

I. INTRODUCTION

In a recent paper[1] Park *et al.* presented a thorough study of oscillatory Couette flows between two parallel smooth walls as an archetypal small-scale oscillatory shear-driven gas flow. These flows have attracted significant interest in recent years in connection to a variety of microelectromechanical system related applications.[2] Using direct Monte Carlo simulations[3] and analytical solutions, Park *et al.* studied a wide range of Knudsen ($\mathrm{Kn}=\lambda/L$) and Stokes ($S=\sqrt{\omega L^2/\nu}$) numbers. Here λ is the molecular mean free path, ω is the oscillation frequency, $\nu=\mu/\rho$ is the gas kinematic viscosity, ρ is the gas density, and L is the characteristic flow length scale, which in this case is the distance between the two walls. Specifically, Knudsen numbers ranged from the slip-flow regime $\mathrm{Kn} \lesssim 0.1$ to the free-molecular-flow regime $\mathrm{Kn} \gtrsim 10$, and two models for describing the gas behavior in certain flow regimes were studied. The first model, referred to as an "engineering model,"[4] is a generalized first-order slip-flow relation augmented by a number of adjustable (fitted) coefficients; the addition of these coefficients enables the model to describe the flow field for all Kn *as long as the flow is quasistatic* ($S \ll 1$), in addition to describing the flow in the $\mathrm{Kn} \lesssim 0.1$ regime. Unfortunately, this adjustable parameter approach removes the ability of the slip model to capture the stress field and thus necessitates the use of a separate fit for the stress. Additionally, fitted slip-flow models are known to be valid only for the flow they have been fitted to; this is explained and rectified below. The second model proposed is a collisionless Boltzmann equation formulation that is solved numerically; the authors show that this model is effective for large Knudsen numbers ($\mathrm{Kn} \gg 1$), as expected.

The purpose of the current paper is twofold: first, we provide a rigorous alternative to the engineering model proposed by Park *et al.* for use in the $\mathrm{Kn} < 1$ limit. In particular, we use a second-order slip model, which is able to capture both the flow field *and* stress field with no fitted/adjustable parameters. The second objective of this paper is to provide closed-form solutions of the free-molecular-flow formulation of Park *et al.* These solutions are parametrized by a "ballistic Stokes number" $S_b=\omega L/c_m$ which, as expected, becomes the relevant nondimensional parameter characterizing the oscillation frequency in this collisionless transport limit. Here $c_m=\sqrt{2kT/m}$ is the most probable molecular speed, T is the gas temperature, k is the Boltzmann's constant, and m is the molecular mass. Our results also provide closed-form descriptions of the bounded shear layer structures reminiscent of Stokes layers observed by Park *et al.* in the high frequency and high Knudsen number limit.

II. PROBLEM DESCRIPTION

We consider a dilute hard-sphere gas between two infinite, fully accommodating, plane walls; the two walls are located at $y=0$ and $y=L$, respectively, and are parallel to the x-z plane. The assumption of full accommodation is motivated by experimental observations[3,5,6] which suggest that for the "engineering" surfaces of interest here, specular reflection levels are very low. The ratio of specific heats of this gas will be denoted by γ. At $t=0$ the wall at $y=0$ starts to oscillate in its own plane and in the x direction with velocity $U=U_0 \sin \omega t$. We are interested in the steady state behavior of this system as described by the velocity of the gas in the x direction $u(y)$ and the shear stress in the gas $\tau_{xy}(y)$. We will assume that U_0 is small enough so that the governing equations and boundary conditions in the kinetic formulation of

Sec. IV can be linearized; this assumption also allows the use of the second-order slip model of Sec. III which is derived from a linearized kinetic formulation. Linear kinetic conditions may be assumed when $U_0 \ll c_m$, that is, when the Mach number based on the wall velocity $[M = U_0/(\sqrt{\gamma/2}c_m)]$ is small.[5] This is not a very restrictive assumption with regard to practical applications. As will be seen below, under linearized conditions the flow is isothermal and so throughout this paper the gas density ρ and temperature T are understood to be constant.

An implication of the linearization condition $U_0 \ll c_m$ stems from the von Karman relation,[7]

$$M = \sqrt{\frac{3\pi}{40}} 1.270 \, \mathrm{Re}\,\mathrm{Kn} \approx \mathrm{Re}\,\mathrm{Kn}, \tag{1}$$

where $\mathrm{Re} = U_0 L/\nu$ is the Reynolds number. Relation (1) implies that any formulation based on the assumption $M \ll 1$ is limited to $\mathrm{Re} \ll 1$ for $\mathrm{Kn} > 0.1$. Although convection is not important in the problem studied here, this discussion aims to clarify that, when referring to second-order slip models and the associated extension of the Navier–Stokes description to $\mathrm{Kn} > 0.1$, the condition $\mathrm{Re} \ll 1$ is implied, because, as stated above, the second-order slip model used here is based on such an assumption ($M \ll 1$). In other words, the term "Navier–Stokes" is used here in a more general sense and is to be understood as generally denoting the set of continuum conservation laws subject to the linear-gradient transport closures appropriate to the $\mathrm{Kn} \ll 1$ limit.

III. SOLUTION FOR Kn<1

Although use of the Navier–Stokes description is usually limited to the no-slip and slip-flow regimes, the recent development of a reliable second-order slip model[8,9] for the hard-sphere gas allows the use of this description well into the transition regime. In Sec. III B we provide an analytical solution of the oscillatory shear problem made possible by the second-order slip model described also below.

A. Second-order slip model

Second-order slip models can, in some cases, extend the range of applicability of the Navier–Stokes description around and beyond $\mathrm{Kn} \approx 0.1$ where the accuracy of first-order slip models begins to deteriorate.[5] Given the simplicity and negligible cost of Navier–Stokes solutions compared to molecular simulations, accurate second-order slip models are very desirable.

For this reason, the author has recently developed and validated[8,9] a rigorous second-order slip model for the hard-sphere gas. This model combines elements of the original asymptotic theory of Cercignani[10] (based on the BGK approximation of the Boltzmann equation) with elements of the later work of Sone and collaborators (also based on the same model equation[7]) to form a second-order slip framework. This framework is then made suitable for the hard-sphere gas by replacing the BGK slip coefficients by appropriate *nonadjustable* values for the hard-sphere gas.[8,9] As discussed before[9] and also below, this last modification holds the key to making this theory useful, because now agreement with realistic Boltzmann simulations and *physical experiments* can be *demonstrated*. We, in fact, believe that the inability of the BGK model to provide this connection to simulations using realistic interaction models or experiments is one of the primary reasons for the lack of interest in the original (BGK) version of the slip-flow theory. This model is now briefly discussed. More details can be found elsewhere.[9]

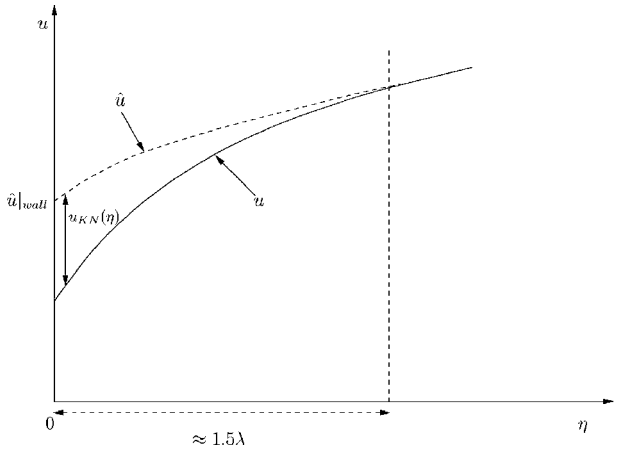

FIG. 1. Schematic of the Knudsen layer in the vicinity of the wall ($\eta = 0$).

Rigorous asymptotic analysis[10] of the BGK model of the Boltzmann equation shows that in steady, one-dimensional flows the appropriate second-order boundary condition is of the form

$$\hat{u}\big|_{\mathrm{wall}} - u_w = \alpha\lambda \left.\frac{\partial \hat{u}}{\partial \eta}\right|_{\mathrm{wall}} - \beta\lambda^2 \left.\frac{\partial^2 \hat{u}}{\partial \eta^2}\right|_{\mathrm{wall}}. \tag{2}$$

Here, η is the coordinate normal to the wall and pointing into the gas and $\hat{u}$ is the fluid velocity in the x direction *as predicted by the Navier–Stokes equations*. Differentiating the Navier–Stokes flow field from the "true" flow field as given by solution of the Boltzmann equation (u) is necessary because within the asymptotic analysis $u = \hat{u} + u_{\mathrm{KN}}$. Here u_{KN} is a kinetic boundary layer contribution, known as the Knudsen layer, which becomes important in the near-wall regions, i.e., $u_{\mathrm{KN}} \to 0$ as $\eta/\lambda \to \infty$[9] (see Fig. 1). In other words, slip-flow boundary conditions provide effective boundary conditions for $\hat{u}$, the *Navier–Stokes component of the true flow field*, while in the near-wall regions the Knudsen layer needs to be superposed to the former to capture u.

In practice, the "effective" thickness of the Knudsen layer for a hard-sphere gas, based on its decay to a few percent of $u_{\mathrm{KN}}(\eta = 0)$, is $\approx 1.5\lambda$.[7,9] Cercignani's study shows that the contribution of the Knudsen layers to the flow is such that the bulk (average) flow velocity ($u_b = 1/L\int_0^L u\, dy$) differs from the slip-corrected Navier–Stokes approximation to the same quantity ($\hat{u}_b = 1/L\int_0^L \hat{u}\, dy$) to $O(\mathrm{Kn}^2)$. Thus, while for $\mathrm{Kn} \lesssim 0.1$ using only $\hat{u}$ to describe the flow is typically sufficient, for $\mathrm{Kn} \gtrsim 0.1$ and when using second-order slip boundary conditions in particular, Knudsen layers need to be quantitatively taken into account. The existence of the Knudsen layer also implies that a successful second-order slip model is one that *does not agree* with Boltzmann equation

solutions within 1.5λ from the walls. This explains why attempts towards determining β by fitting direct simulation Monte Carlo (DSMC) solutions in the entirety of the simulation domain have not led to a predictive model with no adjustable parameters.

In one-dimensional flows, the hard-sphere second-order slip model reduces to Eq. (2) with $\alpha=1.11$ and $\beta=0.61$. This model was shown to be in excellent agreement with direct Monte Carlo solutions of the Boltzmann equation for Kn $\leqslant 0.4$ in the case of pressure-driven flow,[8] a one-dimensional impulsive start problem[9] and an oscillatory shear flow problem.[9] In higher dimensions the second-order term is significantly more complex;[7] also, wall curvature introduces additional terms.[7,12,13] This, in fact, explains why the experimentally measured second-order slip coefficient extracted from pressure-driven flow in tubes is found to differ from the second-order slip coefficient measured from pressure-driven flow in two-dimensional channels.

One aspect of slip-flow theory perhaps not fully appreciated is that slip models are so useful because they do not require modifications to the viscous constitutive relation (e.g., through additional adjustable parameters or variable viscosity constructs). Within the slip-flow asymptotic theory this is manifested by the fact that the stress field does not require a Knudsen layer correction.[9] This paper, as well as previous work,[9] clearly shows that the true (Boltzmann) stress field is correctly captured by the second-order slip model used here.

A final feature of the second-order slip model is that it is possible to quantitatively account for the contribution of the Knudsen layer to the bulk flow speed *without solving the Boltzmann equation*; this is important because Knudsen layers penetrate appreciable parts of the flow as the Knudsen number increases, and consequently the Navier–Stokes velocity prediction deteriorates as Kn grows beyond Kn$\approx$0.2. In a one-dimensional geometry, the bulk flow velocity is given by

$$u_b = \frac{1}{L}\int_0^L u\, dy = \frac{1}{L}\int_0^L \left[\hat{u} + \varepsilon\lambda^2 \frac{\partial^2 \hat{u}}{\partial y^2}\right] dy, \tag{3}$$

where for a hard-sphere gas $\varepsilon=0.296$.[8] A direct consequence of the above relation is that in Poiseuille-type flows where the curvature of $\hat{u}$ is constant, experimental measurement of the flow rate ($u_b L$) yields an "effective" second-order slip coefficient $\beta-\varepsilon$.[9] Recent experiments in helium and nitrogen[14] report a second-order slip coefficient of $\approx 0.25\pm 0.1$ which is in good agreement with the model prediction $\beta-\varepsilon=0.31$. Therefore, this model is also able to provide a resolution of the long-standing discrepancy between experimental data and second-order slip model predictions.

B. Results

The solution of the oscillatory Couette problem in the Navier–Stokes approximation reduces to solution of

$$\frac{\partial \hat{u}}{\partial t} = \nu \frac{\partial^2 \hat{u}}{\partial y^2} \tag{4}$$

subject to the slip-flow boundary conditions

$$\hat{u} - U_0\, \mathrm{Im}[\exp(i\omega t)] = \alpha\lambda \frac{\partial \hat{u}}{\partial y} - \beta\lambda^2 \frac{\partial^2 \hat{u}}{\partial y^2} \quad \text{at } y=0,$$

$$\hat{u} = -\alpha\lambda \frac{\partial \hat{u}}{\partial y} - \beta\lambda^2 \frac{\partial^2 \hat{u}}{\partial y^2} \quad \text{at } y=L.$$

The steady state solution is given by

$$\hat{u} = \mathrm{Im}\left\{\left[A\cosh\left(\zeta\frac{y}{L}\right) + B\sinh\left(\zeta\frac{y}{L}\right)\right]\exp(i\omega t)\right\}, \tag{5}$$

where Im denotes the imaginary part. Here,

$$A = U_0 \frac{D}{(1+\beta\zeta^2\,\mathrm{Kn}^2)D + \alpha\zeta\,\mathrm{Kn}C}, \tag{6}$$

$$B = -\frac{C}{D}A, \tag{7}$$

$$C = \cosh\zeta + \alpha\zeta\,\mathrm{Kn}\sinh\zeta + \beta\zeta^2\,\mathrm{Kn}^2\cosh\zeta, \tag{8}$$

$$D = \sinh\zeta + \alpha\zeta\,\mathrm{Kn}\cosh\zeta + \beta\zeta^2\,\mathrm{Kn}^2\sinh\zeta, \tag{9}$$

and $\zeta=\sqrt{i}S$. One of the quantities of interest is the magnitude of the shear stress on the driven wall $|\tau_{xy}(y=0)|=\tau_w$. From the above solution we obtain

$$\frac{\tau_w}{\mu U_0/L} = \left|\frac{\zeta C}{(1+\beta\zeta^2\,\mathrm{Kn}^2)D + \alpha\zeta\,\mathrm{Kn}\,C}\right|. \tag{10}$$

As discussed above, for sufficiently low speeds the flow is expected to be isothermal. In fact, the argument presented in Sec. IV for the collisionless Boltzmann equation can be generalized in the presence of collisions[11] to show that under the linear conditions assumed here the isothermal assumption is valid. Here we will provide a Navier–Stokes point of view: the isothermal approximation is reasonable when the Brinkman number $\mathrm{Br}=\mu U_0^2/(\kappa T)$ is small, where κ is the thermal conductivity. Using the fact that for a monoatomic gas $\kappa/\mu \approx 15k/(4m)$ we see that $\mathrm{Br}=4mU_0^2/(15kT)=8U_0^2/(15c_m^2)\ll 1$ is automatically satisfied under linear conditions.

IV. SOLUTION IN THE COLLISIONLESS LIMIT

Let $\mathbf{c}=(c_x,c_y,c_z)$ be the molecular velocity vector. By assuming linearized conditions ($U_0 \ll c_m$) we can write the distribution function of molecular velocities as $f=\rho F(1+\phi)$ and neglecting higher order terms in ϕ, we obtain the linearized Boltzmann equation in the collisionless approximation,[1]

$$\frac{\partial \phi}{\partial t} + c_y \frac{\partial \phi}{\partial y} = 0. \tag{11}$$

Here

$$F = \left(\frac{1}{\pi c_m^2}\right)^{3/2} \exp\left(-\frac{c_x^2+c_y^2+c_z^2}{c_m^2}\right) \tag{12}$$

is the equilibrium Maxwellian distribution function. The macroscopic velocity in the x direction is obtained from

$$u = \int c_x \phi F \, d\mathbf{c} \tag{13}$$

when the solution for ϕ is established. The validity of the constant density and temperature assumption can be verified from the solution (to be obtained below) which will be seen to be an odd function of c_x. This property of the solution also means that the mass flux to the wall remains equal to its equilibrium value and thus the linearized boundary conditions at the two walls can be written as[11]

$$\phi = \frac{2c_x U}{c_m^2}, \quad c_y > 0 \quad \text{at } y = 0, \tag{14}$$

$$\phi = 0, \quad c_y < 0 \quad \text{at } y = L. \tag{15}$$

The solution

$$\tilde{\phi} = \frac{2c_x \tilde{U}}{c_m^2} \exp\left(-\frac{sy}{c_y}\right), \quad c_y > 0, \tag{16}$$

$$\tilde{\phi} = 0, \quad c_y < 0 \tag{17}$$

is obtained by using the Laplace transform technique. Here s is the Laplace variable and $\sim$ denotes the Laplace transform of a function. It can be observed that the solution is an odd function of c_x, confirming our *a priori* assumption of isothermal, constant density flow. Using (16) and (17) into (13) we obtain

$$\tilde{u} = \frac{\tilde{U}}{\sqrt{\pi}} \int_{\xi>0} \exp\left[-\left(\xi^2 + \frac{sy}{c_m \xi}\right)\right] d\xi. \tag{18}$$

Taking the inverse Laplace transform of this equation leads to

$$u = \frac{U_0}{\sqrt{\pi}} \int_{y/(c_m t)}^{\infty} \sin\left(\omega t - \frac{\omega y}{c_m \xi}\right) \exp(-\xi^2) d\xi. \tag{19}$$

In steady state the solution is given by

$$u = \frac{U_0}{\sqrt{\pi}} \operatorname{Im}\left\{ \exp(i\omega t) \int_0^{\infty} \exp\left[-\left(\xi^2 + \frac{i\omega y}{c_m \xi}\right)\right] d\xi \right\}. \tag{20}$$

One would expect that "ballistic Stokes layers" will appear in the limit of high "ballistic Stokes number" $S_b = \omega L / c_m$. In this limit the above integral can be approximated using the asymptotic expansion,[15]

$$\int_0^{\infty} \exp\left[-\left(\xi^2 + \frac{\psi}{\xi}\right)\right] d\xi = \sqrt{\frac{\pi}{3}} \exp\left[-3\left(\frac{\psi}{2}\right)^{2/3}\right] \times \left\{1 - \frac{1}{36}\left(\frac{2}{\psi}\right)^{2/3} + \frac{25}{2592}\left(\frac{2}{\psi}\right)^{4/3} + \ldots\right\} \tag{21}$$

suitable for large values of ψ. From this equation, it appears that good approximations can be obtained for $\psi > 2$ by keeping only the first term in the expansion. Thus, for $S_b y/L > 2$ we obtain

$$u = \frac{U_0}{\sqrt{3}} \exp\left[-\frac{3}{2}\left(\frac{S_b}{2}\right)^{2/3}\left(\frac{y}{L}\right)^{2/3}\right] \times \sin\left[\omega t - \frac{3\sqrt{3}}{2}\left(\frac{S_b}{2}\right)^{2/3}\left(\frac{y}{L}\right)^{2/3}\right]. \tag{22}$$

This expression explains recent DSMC results reporting a nonconstant wave speed and a signal decay that is "not exactly exponential."[1]

If we define a ballistic Stokes layer thickness δ to be the distance from the wall to the location where $|u|$ drops to $0.01U_0$, we obtain

$$\delta = \frac{8.9}{S_b} L. \tag{23}$$

Thus, a bounded layer will form for $S_b \gtrsim 10$. Note, however, that this expression assumes the existence of a wall at $y=L$ such that $\mathrm{Kn} \gg 1$. A more general relation can be obtained by writing

$$\delta = \frac{8.9 c_m}{\omega} = \frac{8.9\sqrt{\pi}}{2} \frac{\lambda}{\omega \tau_c}, \tag{24}$$

where $\tau_c = \lambda/\bar{c}$ is the collision time and $\bar{c} = (2/\sqrt{\pi}) c_m$ is the mean molecular speed. We thus expect a ballistic bounded layer will form in a domain of arbitrary length if $\omega \tau_c \gg 10$ (and $L > \delta$). In this case, the relevant length scale is $\delta (\ll \lambda)$ as given above and not L.[1]

To treat the low frequency limit analytically we use a series expansion[15] of integral (20) suitable for $S_b y/L \ll 1$ to obtain

$$u = \frac{U_0}{2}\left[1 - \sqrt{\pi} S_b \frac{y}{L} + S_b^2 \left(\frac{y}{L}\right)^2\right] \sin \omega t - \frac{U_0}{\sqrt{\pi}} S_b \frac{y}{L}\left[1 - \frac{3}{2}\tilde{\gamma} - \ln\left(S_b \frac{y}{L}\right)\right] \cos \omega t, \tag{25}$$

where $\tilde{\gamma} = 0.577\ldots$ is Euler's constant. Retaining up to second-order terms in the expansion leads to an accurate representation of the integral up to $S_b y/L \approx 0.4$.

Finally, the shear stress can be calculated from

$$\tau_{xy} = \rho \int (c_x - u) c_y (1 + \phi) F \, d\mathbf{c} = \rho \int c_x c_y \phi F \, d\mathbf{c} \tag{26}$$

using the appropriate asymptotic expansions.[15] Of particular interest in this case is the magnitude of the shear stress at the driven wall

$$\tau_w^{\mathrm{FM}} = \frac{1}{2} \rho U_0 \sqrt{\frac{2kT}{\pi m}}, \tag{27}$$

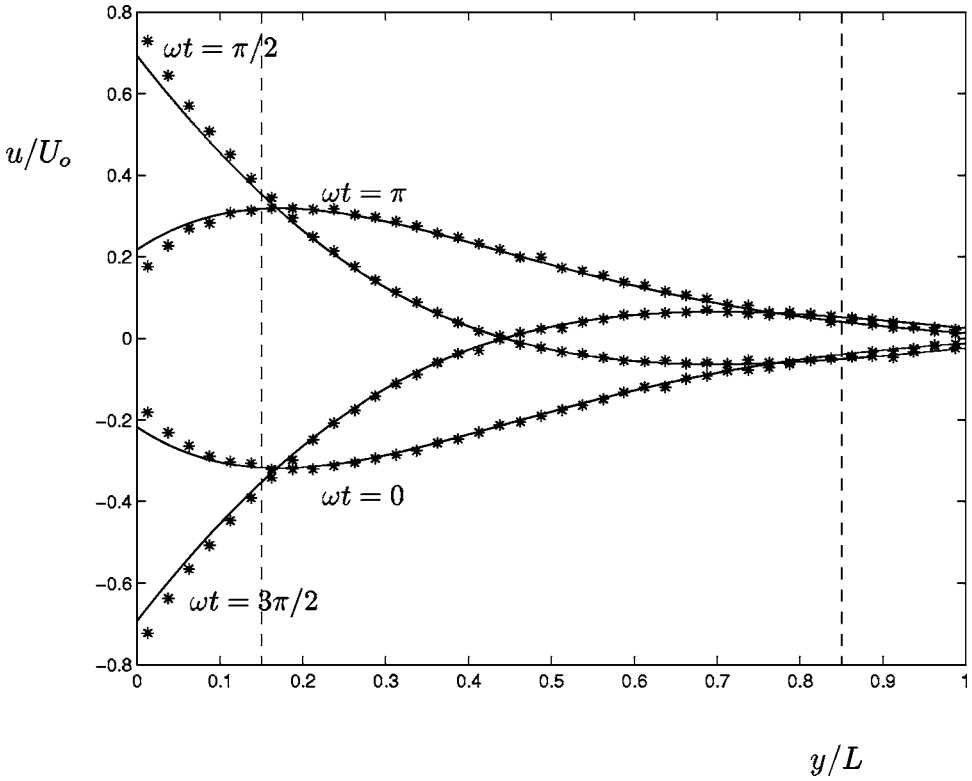

FIG. 2. Velocity profile comparison for Kn=0.1, S=4. The theoretical result [Eq. (5)] obtained using the second-order slip model of Sec. III A is shown as a solid line. DSMC simulations are shown in stars. The dashed vertical lines denote the extent of the Knudsen layer (which starts at the wall), and thus enclose the region where the DSMC result (u) is directly comparable to the Navier–Stokes result ($\hat{u}$).

which is independent of the oscillation frequency and equal to the steady free-molecular value.[1] The superscript FM denotes free molecular. Using Eq. (27) we can write

$$\frac{\tau_w^{\mathrm{FM}}}{\mu U_0/L} = \frac{1}{2\mathrm{Kn}}. \tag{28}$$

V. COMPARISON WITH DSMC SIMULATIONS AND DISCUSSION OF RESULTS

We performed direct Monte Carlo simulations[3] to verify the theoretical results of Secs. III and IV. Standard[16] DSMC techniques were used. Figures 2 and 3 show a comparison

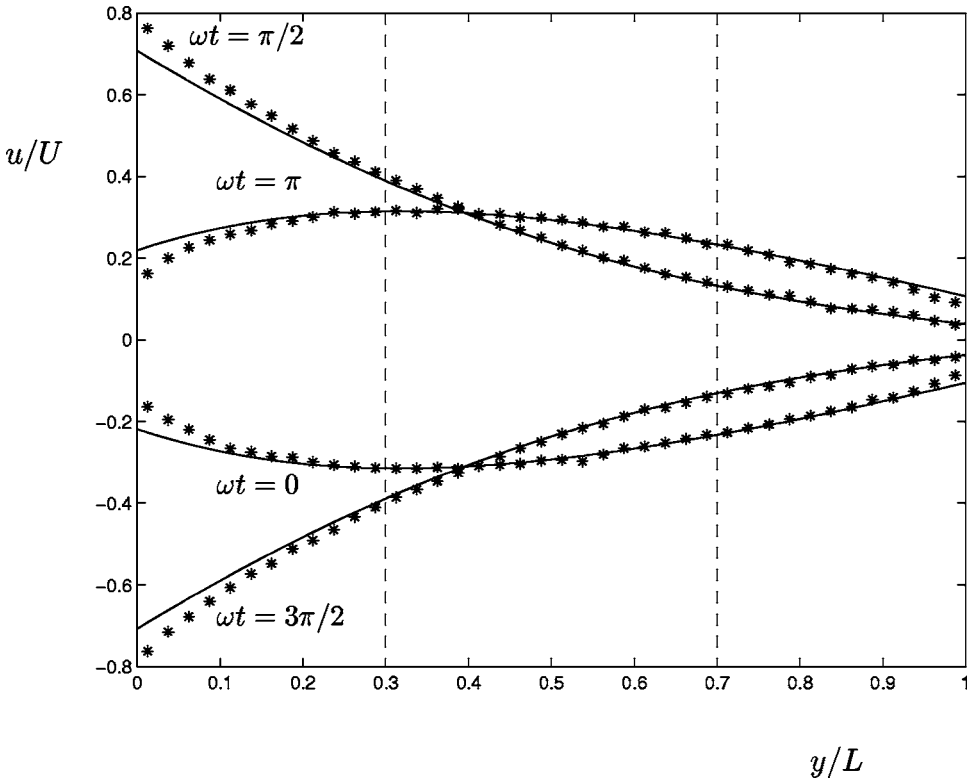

FIG. 3. Velocity profile comparison for Kn=0.2, S=2. The theoretical result [Eq. (5)] obtained using the second-order slip model of Sec. III A is shown as a solid line. DSMC simulations are shown in stars. The dashed vertical lines denote the extent of the Knudsen layer (which starts at the wall), and thus enclose the region where the DSMC result (u) is directly comparable to the Navier–Stokes result ($\hat{u}$).

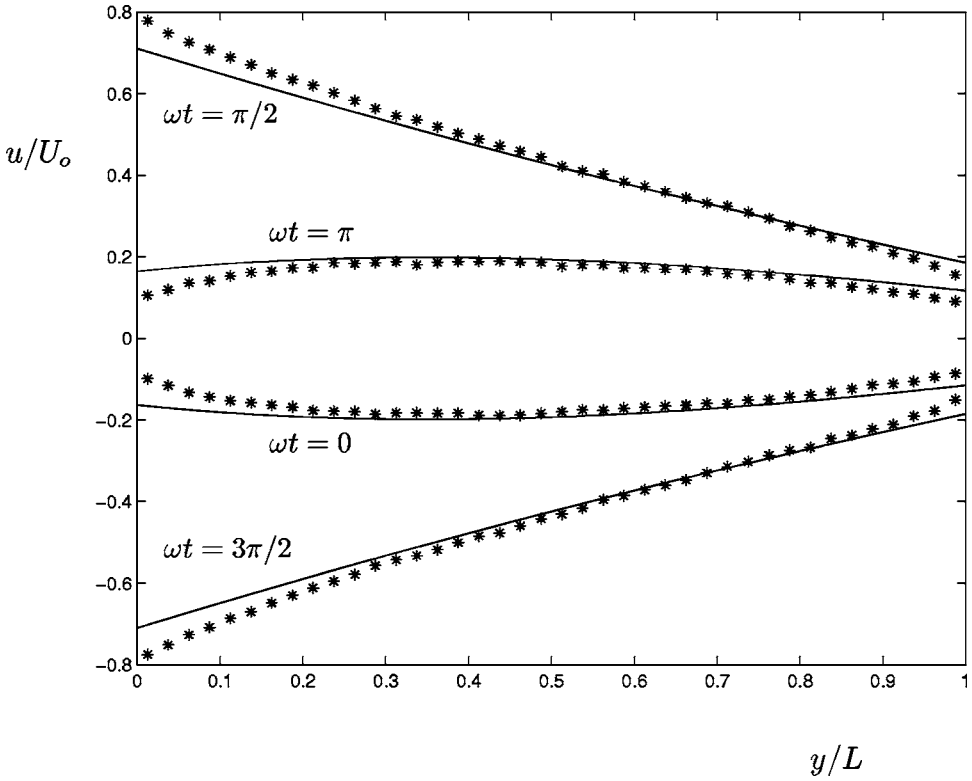

FIG. 4. Velocity profile comparison for $\mathrm{Kn}=0.4, S=1$. The theoretical result [Eq. (5)] obtained using the second-order slip model of Sec. III A is shown as a solid line. DSMC simulations are shown in stars. Kinetic effects are important in the whole computational domain at this Knudsen number making direct comparison between u and $\hat{u}$ difficult.

between DSMC results (u) and those obtained using the second-order slip model ($\hat{u}$). The figures also indicate the width of the Knudsen layer wherein the Navier–Stokes profile ($\hat{u}$) *should not* be expected to match the DSMC solution (u). These figures clearly indicate that part of the challenge in using a second-order slip model lies in the interpretation of results; provided the existense of the Knudsen layer is accounted for, the agreement between the DSMC and NS results is very good.

Interpretation of the results becomes more challenging for $\mathrm{Kn} \gtrsim 0.3$ where $u_{\mathrm{KN}} \neq 0$ everywhere in the physical domain and a Knudsen *layer* becomes difficult to define (see Fig. 4). In this case, knowledge of profile $\hat{u}$ is not sufficient to describe u anywhere in the physical domain. However, the second-order slip model remains *accurate* and useful beyond $\mathrm{Kn} \approx 0.3$. We claim that the second-order slip model remains accurate because it is correctly capturing all quantities that the Navier–Stokes description is expected to describe, namely, $\hat{u}$ and the stress field (for the latter see Fig. 8). The fact that $\hat{u}$ is correctly captured beyond $\mathrm{Kn} \approx 0.3$ is inferred from the fact that when a correction for the Knudsen layer contribution is added to $\hat{u}$ [using Eq. (3)], the bulk flow velocity is in excellent agreement with DSMC results for a number of flows.[9] Although explicit knowledge of u_{KN} would have been preferable, this would require solution of the Boltzmann equation. The value of the second-order slip model discussed here lies in its ability to provide an accurate description of the Navier–Stokes part of the flowfield, the true (Boltzmann) stress field and the average effect of the Knudsen layer [see Eq. (3)] without requiring solution of the Boltzmann equation.

Figure 5 shows a comparison between the theoretical result (22) and DSMC simulations for $\mathrm{Kn}=10, S_b=19.9$. Figure 6 shows a comparison between the theoretical result (22) and DSMC simulations for $\mathrm{Kn}=5, S_b=9.9$. Both figures show that in the $S_b \gg 1$ limit the agreement is very good (except when $y/L \to 0$ as expected) and the effect of molecular collisions appears to be very small. On the other hand, the comparison between the collisionless theory and DSMC simulations in Fig. 7 shows that the effect of collisions is not completely negligible at $\mathrm{Kn} \approx 10$ in the $S_b \ll 1$ limit. This is expected since the very high frequencies ($\omega \tau_c \gg 1$) present for $S_b \gg 1$ have the effect of reducing the importance of molecular collisions.

A comparison between DSMC results and the theoretical results for the wall shear stress is given in Fig. 8. Comparisons for $S=1$, 2, 4 as well as the quasistatic case[1] of $S < 0.25$ for $0.1 \leqslant \mathrm{Kn} \leqslant 20$ were performed. Note that although S ceases to be the relevant parameter for characterizing the oscillation frequency in the high Knudsen number limit, we take advantage of the fact that τ_w is independent of ω (and thus S_b) in this limit to avoid introducing S_b as an additional parameter into the figure. However, it is important to note that the quasistatic results ($S \leqslant 0.25$) have been obtained by steady calculations and thus they correspond to $S_b \ll 1$, while the results for $S=1$, 2, 4 correspond to $S_b \gg 1$. Therefore the results for $S \leqslant 0.25$ support our previous findings [see Fig. 7], namely, that collisions in the $\mathrm{Kn} \gg 1$ limit are more important for $S_b \ll 1$ than for $S_b \gg 1$.

A number of additional observations can be made from Fig. 8: The results show that the second-order slip model of Sec. III accurately captures τ_w up to $\mathrm{Kn} \approx 0.4$ for all S for which the oscillation frequency remains significantly smaller than the molecular collision frequency. In fact, the second-

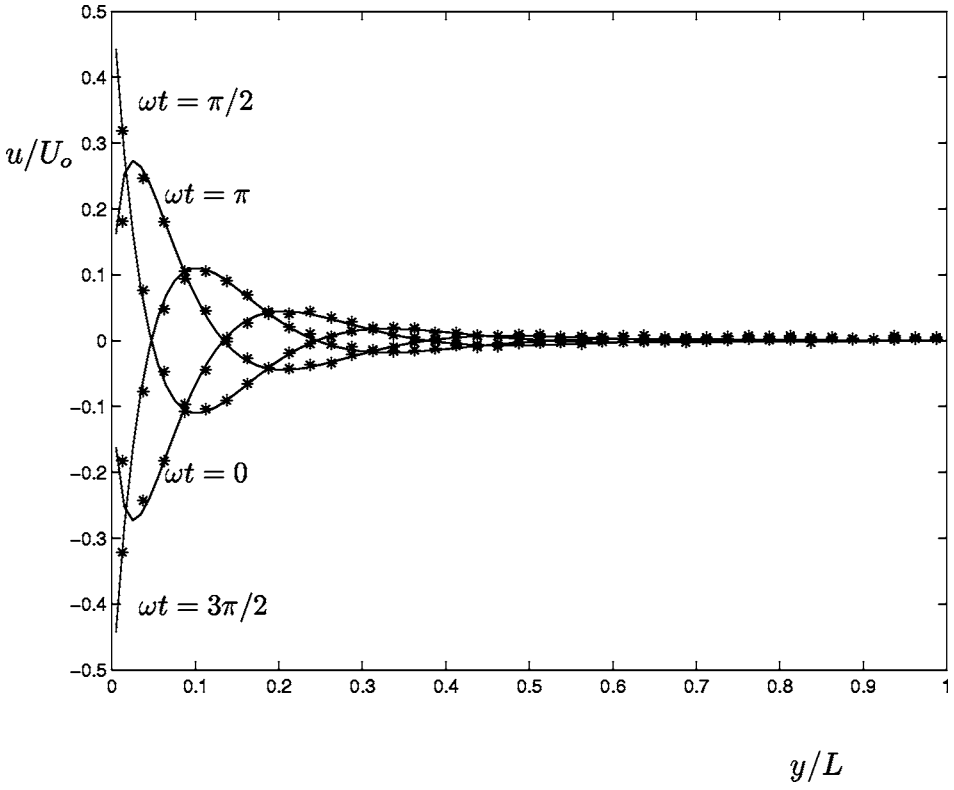

FIG. 5. Velocity profile comparison for Kn=10, S_b=19.9. The theoretical result [Eq. (22)] obtained using the collisionless Boltzmann formulation of Sec. IV is shown as a solid line. DSMC simulations are shown in stars.

order slip model predictions in some cases remain accurate up to Kn$\approx$1. The fact that in steady (and therefore also quasisteady) Couette flows the first-order slip-flow relation describes the stress field fairly accurately has been observed before,[17] and is thought to be due to the simplicity of the problem. At S=1 the curvature present in the flow decreases with increasing Knudsen number; this may explain why the agreement extends to such high Knudsen numbers. For S $>$1 the agreement does not extend beyond Kn$\approx$0.4, but it should also be kept in mind that as S increases the oscillation frequency approaches the molecular collision frequency (S

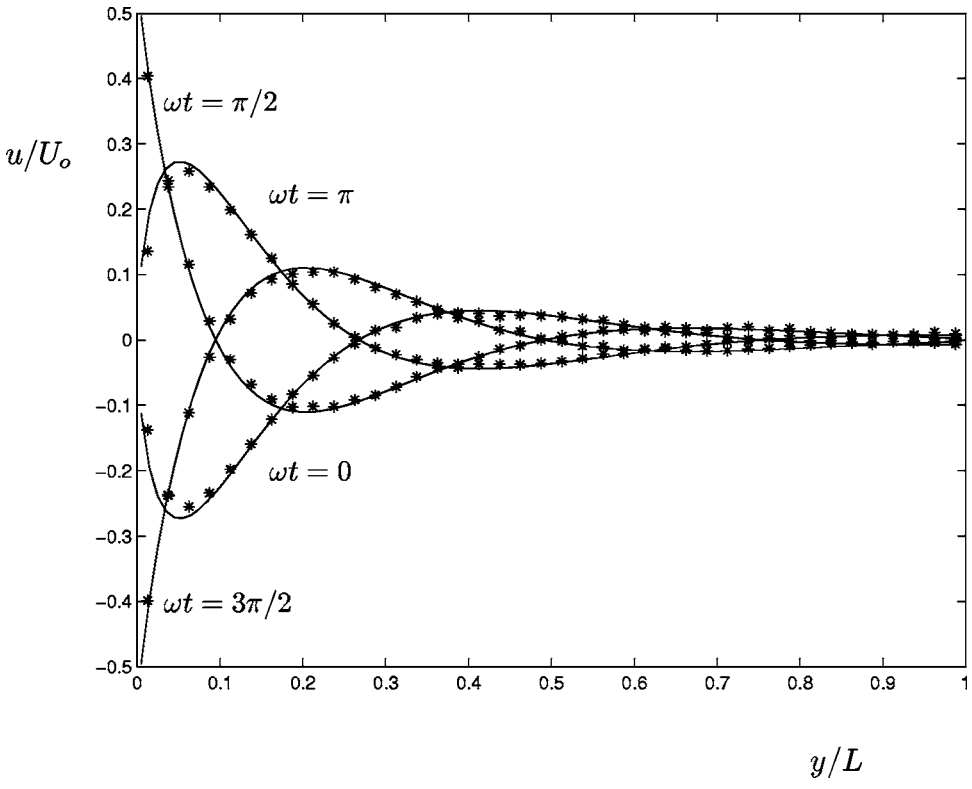

FIG. 6. Velocity profile comparison for Kn=5, S_b=9.9. The theoretical result [Eq. (22)] obtained using the collisionless Boltzmann formulation of Sec. IV is shown as a solid line. DSMC simulations are shown in stars.

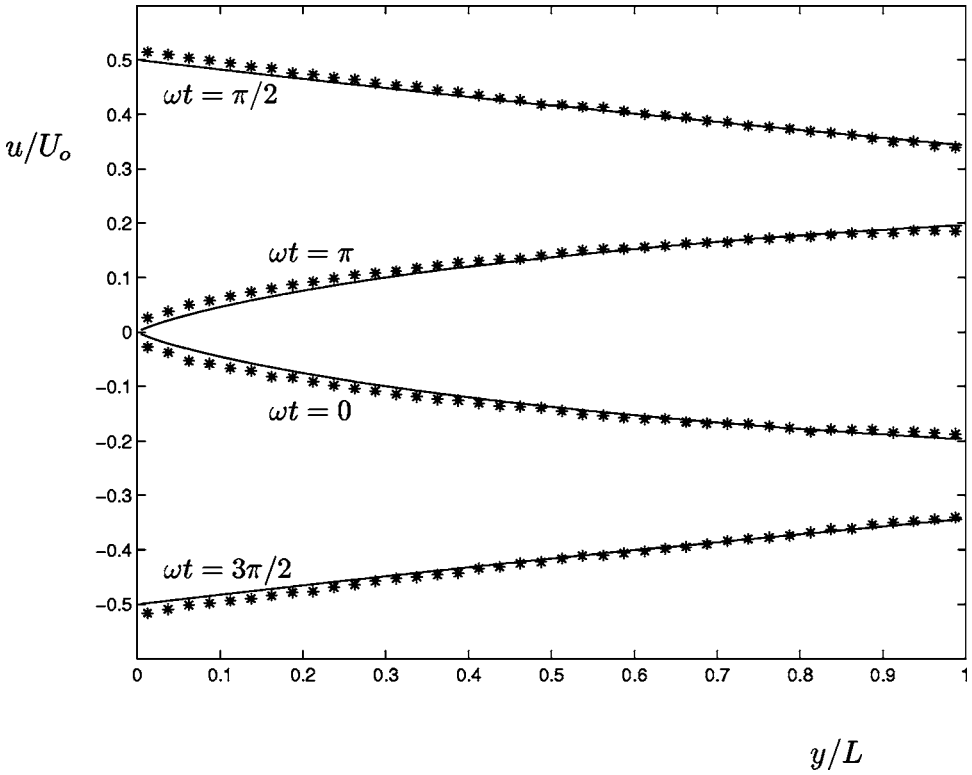

FIG. 7. Velocity profile comparison for $\mathrm{Kn}=10, S_b=0.2$. The theoretical result [Eq. (25)] obtained using the collisionless Boltzmann formulation of Sec. IV is shown as a solid line. DSMC simulations are shown in stars.

$=\sqrt{2\omega\tau_c}/\mathrm{Kn}$).[18] In particular, the conditions $(S=2, \mathrm{Kn}=0.4)$ and $(S=4, \mathrm{Kn}=0.2)$ correspond to $\omega\tau_c=0.32$ while $(S=4, \mathrm{Kn}=0.4)$ corresponds to $\omega\tau_c=1.28$. Given this, it is actually remarkable that the second-order slip model remains reasonably accurate in regimes in which it would normally not be expected to be valid and where alternative solution methods are orders of magnitude more computationally expensive. We also use the data of Fig. 8 to perform a comparison of the present second-order slip model with other such models; this is given in Fig. 9. This figure shows that both Schamberg's $(\alpha=1, \beta=5\pi/12)$ (Ref. 19) and Cercignani's (BGK) $(\alpha=1.1467, \beta=0.9756)$ (Ref. 10) models fail to match the ability of the present model to describe all DSMC data in the relevant $\mathrm{Kn}-S$ parameter space and beyond.

We close by noting that our study serves to demostrate the use and applicability of a second-order model as well as the peculiarities that arise from the existence of a Knudsen

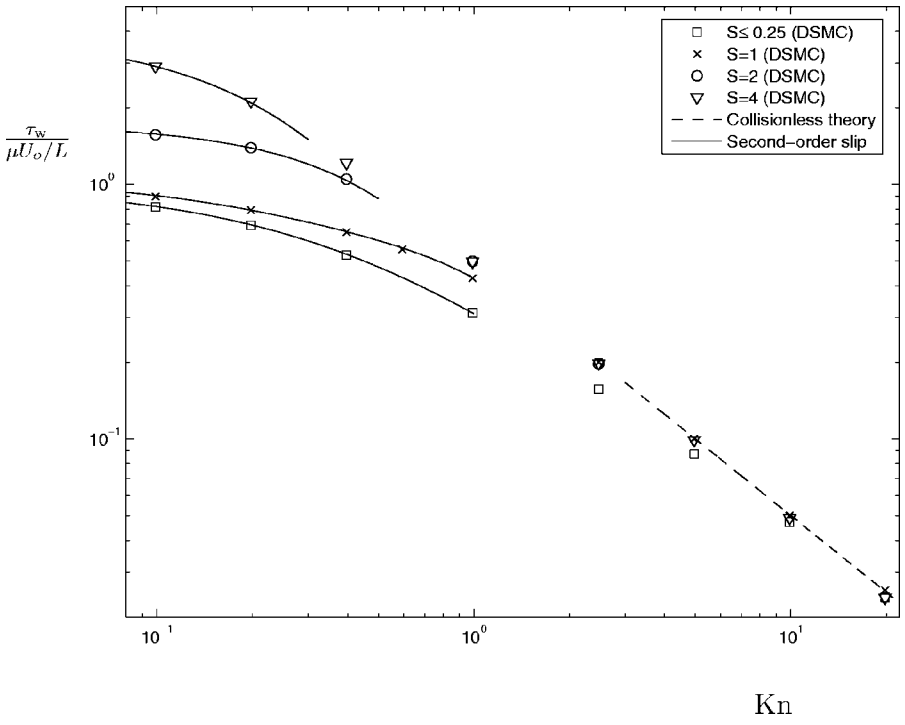

FIG. 8. Normalized wall shear stress magnitude as a function of the Knudsen number. Symbols denote DSMC results. Solid lines denote the second-order slip model result [Eq. (10)]. Dashed line denotes the collisionless result [Eq. (28)]. See text for discussion.

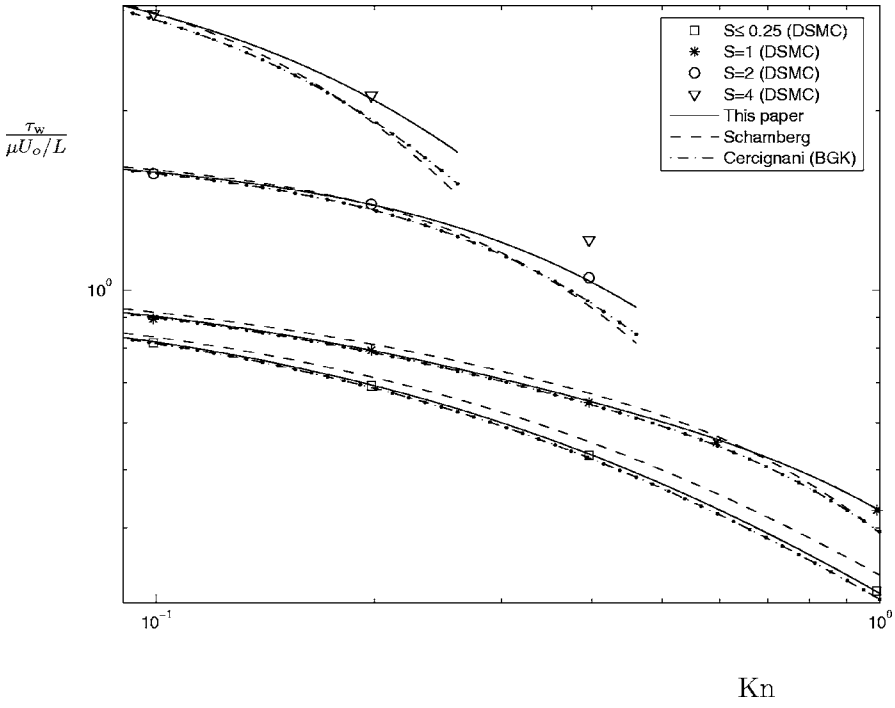

FIG. 9. Normalized wall shear stress as a function of the Knudsen number. Comparison of three second-order slip models.

layer that may not be neglected. Additionally, this study provides a validation of the second-order slip model, providing information on the limits of applicability of this model both in terms of the Knudsen number as well as the proximity of the oscillation frequency to the molecular collision frequency.

ACKNOWLEDGMENTS

The author would like to thank Professor G. Haller and Dr. M. A. Gallis for useful comments and discussions.

[1] J. H. Park, P. Bahukudumbi, and A. Beskok, "Rarefaction effects on shear driven oscillatory gas flows: A DSMC study in the entire Knudsen regime," Phys. Fluids **16**, 317 (2004).
[2] K. S. Breuer, "Lubrication in MEMS," in *The MEMS Handbook*, edited by M. Gad-el-Hak (CRC, Washington, DC, 2002), pp. 1–27.
[3] G. A. Bird, *Molecular Gas Dynamics and the Direct Simulation of Gas Flows* (Clarendon, Oxford, 1994).
[4] P. Bahukudumbi, J. H. Park, and A. Beskok, "A unified engineering model for steady and unsteady shear-driven gas microflows," Microscale Thermophys. Eng. **7**, 291 (2003).
[5] C. Cercignani, *The Boltzmann Equation and its Applications* (Springer, New York, 1988).
[6] T. E. Wenski, T. Olson, C. T. Rettner, and A. L. Garcia, "Simulations of air slider bearings with realistic gas-surface scattering," J. Tribol. **120**, 639 (1998).
[7] Y. Sone, *Kinetic Theory and Fluid Dynamics* (Birkhauser, Boston, 2002).
[8] N. G. Hadjiconstantinou, "Comment on Cercignani's second-order slip coefficient," Phys. Fluids **15**, 2352 (2003).
[9] N. G. Hadjiconstantinou, "Validation of a second-order slip model for dilute gas flows," Microscale Thermophys. Eng. **9**, 137 (2005).
[10] C. Cercignani, "Higher order slip according to the linearized Boltzmann equation," Institute of Engineering Research Report No. AS-64-19, University of California, Berkeley, 1964.
[11] Y. Sone, "Kinetic theory analysis of linearized Rayleigh problem," J. Phys. Soc. Jpn. **19**, 1463 (1964).
[12] D. A. Lockerby, J. M. Reese, D. R. Emerson, and R. W. Barber, "Velocity boundary condition at solid walls in rarefied gas calculations," Phys. Rev. E **70**, 017303 (2004).
[13] R. W. Barber, V. Sun, X. J. Gu, and D. R. Emerson, "Isothermal slip flow over curved surfaces," Vacuum **76**, 73 (2004).
[14] J. Maurer, P. Tabeling, P. Joseph, and H. Willaime, "Second-order slip laws in microchannels for helium and nitrogen," Phys. Fluids **15**, 2613 (2003).
[15] M. Abramowitz, "Evaluation of the integral $\int_0^\infty e^{-u^2-x/u}du$," J. Math. Phys. (Cambridge, Mass.) **32**, 188 (1953).
[16] N. G. Hadjiconstantinou, "Sound wave propagation in transition-regime micro- and nanochannels," Phys. Fluids **14**, 802 (2002).
[17] W. G. Vincenti and C. H. Kruger, *Introduction to Physical Gas Dynamics* (Krieger, Florida, 1965).
[18] N. G. Hadjiconstantinou and A. L. Garcia, "Molecular simulations of sound wave propagation in simple gases," Phys. Fluids **13**, 1040 (2001).
[19] G. E. Karniadakis and A. Beskok, *Micro Flows: Fundamentals and Simulation* (Springer, New York, 2001).